



Dimensional analysis of impulse loading resulting from detonation of shallow-buried charges

Dimensional
analysis

367

Mica Grujicic and Patrick Glomski

*Department of Mechanical Engineering, Clemson University,
Clemson, South Carolina, USA, and*

Bryan Cheeseman

*Army Research Laboratory, Survivability Materials Branch,
Aberdeen Proving Ground, Aberdeen, Maryland, USA*

Received 11 January 2013
Revised 11 January 2013
Accepted 15 April 2013

Abstract

Purpose – Development of military vehicles capable of surviving shallow-buried explosive blast is seldom done using full-scale prototype testing because of the associated prohibitively high cost, the destructive nature of testing, and the requirements for large-scale experimental-test facilities and a large crew of engineers committed to the task. Instead, tests of small-scale models are generally employed and the model-based results are scaled up to the full-size vehicle. In these scale-up efforts, various dimensional analyses are used whose establishment and validation requires major experimental testing efforts and different-scale models. The paper aims to discuss these issues.

Design/methodology/approach – In the present work, a critical assessment is carried out of some of the most important past efforts aimed at developing the basic dimensional analysis formulation for the problem of impulse loading experienced by target structures (e.g. vehicle hull) due to detonation of explosive charges buried to different depths in sand/soil (of different consistency, porosity, and saturation levels).

Findings – It was found that the analysis can be substantially simplified if only the physical parameters associated with first-order effects are retained and if some of the sand/soil parameters are replaced with their counterparts which better reflect the role of soil (via the effects of soil compaction in the region surrounding the explosive and via the effects of sand-overburden stretching and acceleration before the associated sand bubble bursts and venting of the gaseous detonation products takes place). Once the dimensional analysis is reformulated, a variety of experimental results pertaining to the total blast impulse under different soil conditions, charge configurations, charge deployment strategies, and vehicle ground clearances are used to establish the underlying functional relations.

Originality/value – The present work clearly established that due to the non-dimensional nature of the quantities formulated, the established relations can be utilized across different length scales, i.e. although they are obtained using mainly the small-scale model results, they can be applied at the full vehicle length scale.

Keywords Blast impulse loading, Dimensional analysis, Shallow-buried explosive detonation

Paper type Research paper

1. Introduction

Recent efforts of the US Army have been aimed at becoming more mobile, deployable, and sustainable while maintaining or surpassing the current levels of lethality and survivability. Current battlefield vehicles have reached in excess of 70 tons due to ever-increasing lethality of ballistic threats which hinders their ability to be readily transported and sustained. Therefore, a number of research and development



Report Documentation Page

Form Approved
OMB No. 0704-0188

Public reporting burden for the collection of information is estimated to average 1 hour per response, including the time for reviewing instructions, searching existing data sources, gathering and maintaining the data needed, and completing and reviewing the collection of information. Send comments regarding this burden estimate or any other aspect of this collection of information, including suggestions for reducing this burden, to Washington Headquarters Services, Directorate for Information Operations and Reports, 1215 Jefferson Davis Highway, Suite 1204, Arlington VA 22202-4302. Respondents should be aware that notwithstanding any other provision of law, no person shall be subject to a penalty for failing to comply with a collection of information if it does not display a currently valid OMB control number.

1. REPORT DATE

2013

2. REPORT TYPE

3. DATES COVERED

00-00-2013 to 00-00-2013

4. TITLE AND SUBTITLE

Dimensional analysis of impulse loading resulting from detonation of shallow-buried charges

5a. CONTRACT NUMBER

5b. GRANT NUMBER

5c. PROGRAM ELEMENT NUMBER

6. AUTHOR(S)

5d. PROJECT NUMBER

5e. TASK NUMBER

5f. WORK UNIT NUMBER

7. PERFORMING ORGANIZATION NAME(S) AND ADDRESS(ES)

Clemson University, Department of Mechanical Engineering, 241 Engineering Innovation Building, Clemson, SC, 29634-0921

8. PERFORMING ORGANIZATION REPORT NUMBER

9. SPONSORING/MONITORING AGENCY NAME(S) AND ADDRESS(ES)

10. SPONSOR/MONITOR'S ACRONYM(S)

11. SPONSOR/MONITOR'S REPORT NUMBER(S)

12. DISTRIBUTION/AVAILABILITY STATEMENT

Approved for public release; distribution unlimited

13. SUPPLEMENTARY NOTES

14. ABSTRACT

Purpose ? Development of military vehicles capable of surviving shallow-buried explosive blast is seldom done using full-scale prototype testing because of the associated prohibitively high cost, the destructive nature of testing, and the requirements for large-scale experimental-test facilities and a large crew of engineers committed to the task. Instead, tests of small-scale models are generally employed and the model-based results are scaled up to the full-size vehicle. In these scale-up efforts various dimensional analyses are used whose establishment and validation requires major experimental testing efforts and different-scale models. The paper aims to discuss these issues. Design/methodology/approach ? In the present work, a critical assessment is carried out of some of the most important past efforts aimed at developing the basic dimensional analysis formulation for the problem of impulse loading experienced by target structures (e.g. vehicle hull) due to detonation of explosive charges buried to different depths in sand/soil (of different consistency, porosity, and saturation levels). Findings ? It was found that the analysis can be substantially simplified if only the physical parameters associated with first-order effects are retained and if some of the sand/soil parameters are replaced with their counterparts which better reflect the role of soil (via the effects of soil compaction in the region surrounding the explosive and via the effects of sand-overburden stretching and acceleration before the associated sand bubble bursts and venting of the gaseous detonation products takes place). Once the dimensional analysis is reformulated, a variety of experimental results pertaining to the total blast impulse under different soil conditions, charge configurations, charge deployment strategies, and vehicle ground clearances are used to establish the underlying functional relations. Originality/value ? The present work clearly established that due to the non-dimensional nature of the quantities formulated, the established relations can be utilized across different length scales i.e. although they are obtained using mainly the small-scale model results, they can be applied at the full vehicle length scale.

15. SUBJECT TERMS

16. SECURITY CLASSIFICATION OF:			17. LIMITATION OF ABSTRACT Same as Report (SAR)	18. NUMBER OF PAGES 24	19a. NAME OF RESPONSIBLE PERSON
a. REPORT unclassified	b. ABSTRACT unclassified	c. THIS PAGE unclassified			

Standard Form 298 (Rev. 8-98)
Prescribed by ANSI Std Z39-18

programs are under way to engineer light-weight, highly mobile, transportable and lethal battlefield vehicles with a target weight under 20 tons. To attain these goals, significant advances are needed in the areas of light-weight materials and structures as well as in the areas of measurements and prediction of impulse loads resulting from various threats (e.g. IEDs, buried charges, etc.). The present work focuses on the problem of quantifying and predicting impulse loads resulting from buried charges under different soil conditions, charge configurations, charge deployment strategies, and vehicle ground clearances.

The main issue with the detonation-impulse loading measurement efforts is that they should ideally involve full-scale prototypes of the vehicles, which is quite expensive and requires large-scale test facilities and a large crew of engineers committed to the task. On the other hand, it is quite advantageous to carry out all experimental testing and validation using small-scale models and to then scale-up the model results to the full-scale prototype using the appropriate dimensional analysis (defined in the following paragraph).

The main objective of the present work is to critically assess and reformulate the scaling analysis of Wenzel and Hennessey (1972) for military vehicle-hull floor plates subjected to impulse and high-pressure loads associated with detonation of charges shallow-buried in soil under the vehicle hull. The dimensional analysis of Wenzel and Hennessey (1972) is based on the so-called Buckingham *II* theorem (Buckingham, 1914), a procedure commonly used in the situations in which full-scale structures/prototypes are designed and sized based on the results obtained using small-scale model tests. Within the critical assessment stage, each physical parameter (originally identified by Wenzel and Hennessey (1972) as being relevant to the problem at hand) is re-examined with respect to its ability to provide a first-order effect to the impulse loading on a target plate (a surrogate for a vehicle hull). In the dimensional-analysis reformulation stage, an attempt was made to establish a functional relationship between the total charge-detonation impulse and various parameters related to different soil conditions, charge configurations, charge deployment strategies, and vehicle ground clearance.

The main role of the military-vehicle hull floor is to protect the vehicle occupants in the case of shallow-buried charge detonation underneath the vehicle belly. Complex interrelationships generally exist between the type and the extent of vehicle-occupants injuries and the extent of vehicle damage resulting from under-the-vehicle shallow-buried explosive (SBE) blast. The most serious vehicle-occupants injuries and their fatalities are usually incurred as a consequence of hull-floor rupture. In addition to generating floor-material fragmentation, floor rupture enables the ingress of flame and toxic (detonation-product) gases and can lead to on-board fires and explosions. While the vehicle under shallow-buried charge attack is always subjected to high "G" forces, this aspect of the threat is usually considered as secondary when floor rupture takes place. On the other hand, when SBE detonation results in only hull-floor bulging, the vehicle is then propelled upward and off the ground to an extent which scales directly with size of the explosive and inversely with vehicle weight. The accompanying dynamic shock can cause vehicle occupants and on-board instruments and weapons to be thrown about within the vehicle interior. In addition, large hull-floor deflections and deformations can cause a sequence of failures throughout the entire vehicle through components/sub-system connections and interfaces (e.g. via fuel lines running along the floor, floor-bolted seats, ammunition storage racks, power-train lines, etc.).

Traditionally, the floor-rupture problem is solved through the use of thicker floor-plates, stronger, tougher, and usually heavier material and through the utilization of applique armor. This approach is generally associated with unnecessarily oversized/overweight vehicle-hull floors and is being abandoned nowadays due to aforementioned military's requirements for lighter vehicles.

It is clear based on the discussion presented in the previous paragraph that in order to assist vehicle designers in the development of lightweight, high-survivability vehicle hulls, it is critical to be able to accurately measure and correlate the charge-detonation impulse with various parameters pertaining to different soil conditions, charge configurations, charge deployment strategies, and vehicle ground clearances. These measurements and correlations should be applicable at the full vehicle-hull length scale as well as at the length scale of smaller models. The latter requirement clearly suggests that the results of the impulse measurements and their correlations with various parameters related to different soil conditions, charge configurations, charge deployment strategies, and vehicle ground clearance should be defined using non-dimensional quantities which transcend different length scales. In other words, dimensional analysis must be employed. The employment of dimensional analysis in correlating impulse loads resulting from detonation of shallow-buried charges with various parameters pertaining to different soil conditions, charge configurations, charge deployment strategies, and vehicle ground clearance is the main objective of the present work. While employing the dimensional analysis mentioned above, three sets of experimental data were utilized covering a large range of target plate sizes. Details regarding the test setups and procedures used to collect these data sets are presented in Section 3.

It is hoped that application of the proposed dimensional analysis and the associated relations between the physical parameters governing the problem at hand can help vehicle designers reduce the weight of the vehicles while ensuring the required confidence level for vehicle survivability and survivability of vehicle occupants.

The organization of the paper is as follows: overviews of the Buckingham *II* theorem (Buckingham, 1914) and the Wenzel and Hennessey (1972) dimensional analysis are presented in Sections 2.1 and 2.2, respectively, while the proposed reformulation of the latter analysis is discussed in Section 2.3. A brief description of the experimental setups and procedures used to generate the data needed to establish the basic functional relationship between the blast impulse and various soil conditions, charge configurations, charge deployment strategies, and vehicle ground clearances is provided in Section 3. The main results obtained in the present work are presented and discussed in Section 4, while the key conclusions resulted from the present study are summarized in Section 5.

2. Background, critical assessment and reformulation

2.1 Buckingham *II* theorem

As discussed earlier, the Buckingham *II* theorem (also known as "dimensional analysis") (Buckingham, 1914) is employed in the present work in order to address the problem of scale-up of the model results to the full-scale prototype. In the remainder of this section, a brief overview is provided of dimensional analysis and of its utility and limitations.

Dimensional analysis is essentially a technique/procedure for describing the behavior of a system in terms of a number of dimensionless parameters (generally referred to as the Π terms). This procedure typically involves the following main steps:

- (a) Identification of all physical parameters which govern the behavior of the system under investigation. This is the most critical step in the dimensional analysis since it requires a good understanding of the underlying physics of the problem at hand (even in the case when the functional forms of the governing equations are not known).
- (b) Specification of the units for the physical parameters defined in (a) in terms of the fundamental physical dimensions (typically force, length, and time or mass, length, and time).
- (c) Identification of a subset of parameters among the physical parameters defined in (a) with the number of parameters in this subset being equal to the number of fundamental physical dimensions defined in (b). The parameters in this subset will be used for converting the remaining parameters in (a) into a set of dimensionless parameters (i.e. the Π terms). In the case where force/length/time or mass/length/time are the fundamental physical dimensions, there are three physical parameters in this subset. It should be noted that, while in a given problem the number of the resulting Π terms is uniquely defined (equal to the number of physical parameters in (a) minus the number of fundamental dimensions in (b)), the functional form of the Π terms changes with the choice of the physical parameters defining the subset defined earlier. Furthermore, it should be recognized that while it is generally advantageous to define the Π terms in such a way that they have a clear physical meaning, regardless of the choice of the Π terms, the final implications/findings offered by dimensional analysis is independent of the expressions chosen for the Π terms (provided, all the governing physical parameters are correctly identified in (a)).
- (d) Identification of the functional relationships between each of the Π terms and all other Π terms. These relations are generally determined using experimental or computational approaches or the combination of the two approaches.

The power of dimensional analysis is that the functional relations offered are generalized, i.e. the effect of geometrical, kinematic, ambient, loading and response scales is eliminated. Consequently, the dimensional analysis predicts that, if all the pertinent physical parameters were correctly identified in (a) and if all the Π terms were kept invariant (i.e. unchanged) between a small-scale model and its full-scale prototype, then the results obtained using a small-scale model could be directly used to predict the response of the corresponding full-scale counterpart. The condition under which the Π terms are kept invariant is generally referred to as "Similitude Theory".

2.2 Brief overview of Wenzel and Hennessey (1972) work

As mentioned earlier, one of the main objectives of the present work is to critically assess and, if required, reformulate the dimensional analysis presented by Wenzel and Hennessey (1972). In the remainder of this section, a brief overview is provided of the dimensional analysis of Wenzel and Hennessey (1972).

The work of Wenzel and Hennessey (1972) deals with scaling floor-plates for military vehicles expected to be targeted by SBE blast. The main objective of the work was to develop and validate a dimensional analysis for the vehicle floor plate sizing problem, so that the results of small-scale replica-models can be used to determine the minimal required floor-plate thickness which will ensure that, under the specific shallow-buried charge-detonation scenario, the vehicle floor will not undergo rupture or extensive dynamic deflection. The term “replica-model” will be defined in greater detail later in this section. Until then, this term will be used to denote a small-scale model which is similar (geometrically, constitutively, and with respect to extent of properly scaled loads and structural responses) to the corresponding full-scale prototype.

The starting point in the work of Wenzel and Hennessey (1972) was to take advantage of the fact that floor-plate deflections do not significantly modify the (SBE detonation induced) dynamic loading. Toward that end, the problem at hand was divided (decoupled) into two separate problems:

- (1) a floor-plate structural response problem; and
- (2) the problem of analyzing pressures and impulses resulting from detonation of an explosive (shallow buried in soil underneath the vehicle-hull bottom).

2.2.1 Structural response. In their work, Wenzel and Hennessey (1972) carried out a careful and detailed engineering analysis of the structural response of a thick metal plate (a model for the vehicle-hull bottom) supported on wooden blocks (to obtain the required level of ground clearance), and clamped along its edges (to simulate the effect of the surrounding/supported vehicle-frame structure). A schematic of a typical test structure used by Wenzel and Hennessey (1972) is shown in Figure 1.

Physical parameters. The analysis of Wenzel and Hennessey (1972), mentioned above, yielded 11 key physical parameters which govern the response of the plate subjected to SBE detonation loading. These parameters are listed and explained and their fundamental dimensions are identified in Table I. In addition, they are grouped in accordance to their type (e.g. input blast loading, geometrical, material, response). The parameters which define the loading due to SBE blast are the (maximum) pressure, P , and specific impulse, I . Only the case of rectangular target plates was considered and, hence, the physical parameters defining plate geometry include thickness, h , and the two edge lengths, L_1 and L_2 . The constitutive and inertial

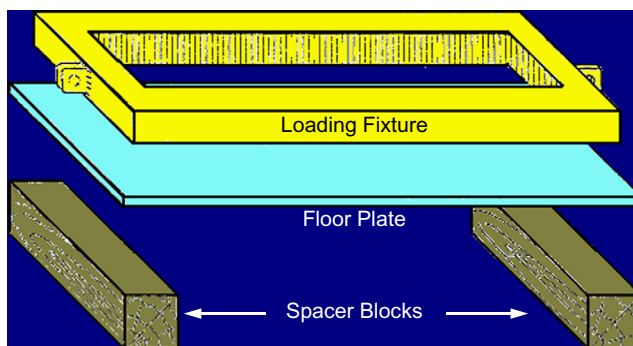


Figure 1.
A schematic of the
prototype SBE-blast
test set-up used in the
work of Wenzel and
Hennessey (1972)

Symbol	Parameter	Fundamental dimensions	Comments
<i>Input blast-loading parameters</i>			
P	Blast pressure	F/L^2	For the rigid-plate case, the pressure can be directly related to the specific impulse and, hence, is an irrelevant parameter
I	Blast specific impulse	FT/L^2	This quantity was not directly measured in the present work and, hence, was eliminated. Please see Table II for more details
<i>Plate geometrical parameters</i>			
h	Plate thickness	L	Not important in the rigid-plate case
L_1, L_2	Rectangular target-plate edge lengths	L	Control the fraction of detonation momentum transferred to the plate. L_1 is equal to L_2 in the case of a square plate
<i>Plate material parameters</i>			
σ	Plate material yield strength	F/L^2	Not important in the rigid-plate case
σ_i	Array of other strength parameters for plate material	–	Not important in the rigid-plate case
ε	Plate material equivalent strain/ductility	–	Not important in the rigid-plate case
ρ	Plate material density	FT^2/L^4	Not important in the rigid-plate case
<i>Plate response parameters</i>			
δ	Plate (bending) deflection	L	Not applicable in the rigid-plate case
a	Plate acceleration	L/T^2	Related to the blast loading pressure and, hence, is also irrelevant
v	Initial velocity after complete momentum transfer	L/T	These two quantities were initially considered as they are directly related to the impulse measurement methods employed in the present work. However, since they scale with the blast impulse, they are not used in this analysis
H	Plate maximum height	L	The need for this quantity appears unclear, difficult to justify, and hence, is not utilized in the present analysis
t	Post-SBE detonation time	T	

Table I. Critical assessment of key physical parameters controlling structural response of the plates originally proposed by Wenzel and Hennessey (1972) and the introduction of additional parameters

response of the target-plate material is characterized by its yield strength, several additional stress-type parameters (e.g. young's modulus, ultimate tensile strength, etc.), σ_i , ductility, ε , and mass density, ρ . The deformation/motion response of the target plate is represented using the maximum flexural displacement, δ and the target plate acceleration, a . Finally, the post-detonation time, t , was added as the last target plate structural response parameter.

Π terms. Next, Wenzel and Hennessey (1972) used a subset of parameters consisting of the plate material yield strength, σ , the plate thickness, h , and the plate material density, ρ , to non-dimensionalize the remaining physical parameters listed above, creating eight Π terms.

Scaling. Finally, within the structural response portion of the problem, Wenzel and Hennessey (1972) established the basic scaling law which enables the use of small-scale models to obtain results applicable to a full-scale prototype. According to this scaling law, if the linear geometry of the target-plate model is scaled by a factor λ with respect to the full-scale structure while the overall shape of the plate and the plate material are kept constant, the model plate deflection will scale with λ , the maximum blast pressure will remain constant, and the specific impulse will scale with $1/\lambda$. In accordance with the previous discussion regarding similitude theory, when the model is constructed in such a way that it complies with this scaling law (i.e. when the model is a so-called “replica-model”), then the model-based test results can be directly applied to the full-scale prototype if each Π term remains unchanged between the two length scales. In other words, both the model and the prototype designs are associated with a same point in the multi-dimensional Π space and the knowledge of a functional relationship between the Π terms is not needed.

2.2.2 SBE detonation induced impulses and pressures. Wenzel and Hennessey (1972) also carried out a detailed engineering analysis of detonation of explosives shallow-buried in soil. In order to quantify the resulting time-dependant impulses and pressures (input loading parameters in the structural response analysis), they included the effect of the explosive shape, size, and type, as well as properties of soil and the surrounding (ambient) air.

SBE related parameters. The analysis of Wenzel and Hennessey (1972), mentioned above, yielded 13 key physical parameters which govern the loadings produced by a SBE detonation. These parameters along with their fundamental dimensions are listed in Table II. In addition, they are grouped in accordance to their type (e.g. charge, charge/plate positioning, ambient air, soil, blast loading, etc.). The SBE was considered to be of a circular-disk shape and to have a size defined by thickness, t , and radius, r . The type of explosive is then expressed by the total energy released during SBE detonation, E . The location of the explosive with respect to the model/prototype is defined in terms of the depth-of-burial, d (a distance between the top surface of the SBE and the soil/air interface) and standoff distance, R (distance between the top surface of the charge and the bottom of the test plate). To account for the effects of air blast, three ambient-air parameters are considered: ambient pressure, P_o , sound speed in air, a_o , and a ratio of the constant-pressure and constant-volume specific heats in air, γ_o . To account for the effect of soil (into which the explosive is buried) Wenzel and Hennessey (1972), assumed that detonation of a SBE can be related to the problem of landmine detonation and the resulting crater formation. Consequently, they assumed that two soil-specific parameters should be included: the (initial) soil density, ρ , and its seismic velocity, c . Two parameters are introduced associated with the SBE-detonation specific impulse, I , and the associated (peak) pressure, P . Lastly, the effects of gravity are included through consideration of the gravitational acceleration, g , as one of the physical parameters.

Π terms. Next, Wenzel and Hennessey (1972) used a subset of parameters consisting of the standoff distance, R , the explosive internal energy, E , and the seismic velocity, c , to non-dimensionalize the remaining physical parameters listed above, creating ten Π terms.

Symbol	Parameter	Fundamental dimensions	Comments
<i>SBE blast-loading output parameters</i>			
P	Pressure due to SBE blast	F/L^2	For the rigid-plate case, the pressure can be directly related to the specific impulse and, hence, is an irrelevant parameter
I_{sp}	Specific impulse due to SBE blast	FT/L^2	This quantity was not directly measured in the present work and, hence, was eliminated
I	Total blast impulse	FT	A new quantity added to comply with impulse measurement methods employed in the present work
<i>Charge parameters</i>			
E	SBE blast released energy	FL	Retained in the present analysis
t	Circular-disc shape SBE thickness	L	Is not expected to have a first-order effect
r	Circular-disc shape charge radius	L	Controls the volume of soil overburden ejected
v_{det}	Explosive detonation velocity	L/T	A new quantity added which controls the time of sand-overburden bubble burst
<i>Charge/plate positioning parameters</i>			
d	SBE depth of burial	L	Retained in the present analysis
R	SBE/plate standoff distance	L	Retained in the present analysis
<i>Ambient air properties</i>			
P_0	Ambient atmospheric pressure	F/L^2	Are not expected to have a first-order effect since momentum transfer via air shock is relatively small
a_0	Speed of sound in air	L/T	
γ_0	Ratio of specific heats for air	–	
<i>Soil properties</i>			
ρ	Density of soil	FT^2/L^4	Is not expected to have a first-order effect because the soil fracture strain (controls the onset of bubble burst and venting) and irreversible-compaction bulk modulus (controls the absorption of detonation energy by the soil surrounding the charge) play a more important role
c	Seismic velocity	L/T	Controls the volume/depth of compacted soil surrounding the detonated explosive
ϵ_{fr}	Soil fracture strain	–	A new quantity added which controls the onset of sand-overburden bubble burst and venting. For the same type of soil, it may be related to the soil porosity and/or degree of saturation;
K_{ic}	Soil irreversible compaction bulk modulus	F/L^2	A new quantity added which controls the amount of energy absorbed by the soil directly surrounding the charge during irreversible compaction. For the same type of soil, it may be related to the soil porosity and/or degree of saturation

Table II. Critical assessment of key physical parameters defining loading from a SBE originally proposed by Wenzel and Hennessey (1972) and the introduction of additional parameters

(continued)

Symbol	Parameter	Fundamental dimensions	Comments
α	Soil porosity	–	New quantities added which control the maximum degree of compaction
β	Degree of saturation	–	
<i>Gravity</i>			
g	Gravitational acceleration	L/T^2	Due to small travel times and extremely high detonation products/soil ejecta velocities, gravity is not expected to have a first-order effect

Table II.

Scaling. As in the case of the structural response portion of the problem, Wenzel and Hennessey (1972) established the basic scaling law for the SBE impulse-loading portion of the problem which enables the use of small-scale models to obtain results applicable to a full-scale prototype. According to this scaling law, if the linear dimensions of the charge and its position relative to the plate are scaled by λ (the same scaling factor used in the structural response portion of the problem), while the overall shape of the charge as well as the ambient air and soil properties are kept constant and gravity is scaled by $1/\lambda$, then the maximum blast pressure will remain constant and the specific impulse will scale with $1/\lambda$ (as required by the structural response portion of the problem). In accordance with the previous discussion regarding the use of replica models in the structural response portion of the problem, if each Π term is held invariant between the two length scales, then the model-based results can be directly applied to a full-scale case and no knowledge of a functional relationship between the Π terms is needed.

2.2.3 *Critical assessment and reformulation of Wenzel and Hennessey's (1972) dimensional analysis.* The main objective of the work presented in this section is to:

- critically assess the dimensional analysis of Wenzel and Hennessey (1972) in order to identify the physical parameters which are expected to have a first-order effect on the impulse loading resulting from SBE detonation; and
- to reformulate the analysis, if necessary, in order to introduce Π terms whose functional forms have a physical basis and, consequently, will facilitate the establishment of the fundamental relationships between them.

A brief summary of the results obtained in this section is provided in Tables I and II while a more detailed description of the work carried out is provided in the following two subsections.

It should be recognized that within the experimental test procedures utilized within the present work to establish the basic functional relations between Π terms, the target plate used was thick enough that the plate response to the blast loads was dominated by the rigid-body motion. In other words, no significant flexion or damage was incurred by the target plate. Consequently, the identification of the physical parameters with first-order effects was carried out under the rigid target-plate assumption.

Critical assessment. It should be noted that the parameters identified below as being irrelevant or unimportant have not been considered further in the present analysis. Conversely, the parameters identified as having a first-order effect have been retained:

- *Blast pressure.* For the rigid-plate case, this quantity can be directly related to the specific impulse and, hence, is an irrelevant parameter.
- *Blast specific impulse.* This quantity was not directly measured in the present work and, hence, was eliminated and replaced with the total impulse delivered to the target plate.
- *Plate thickness.* Not important under the rigid-plate assumption.
- *Rectangular target-plate edge lengths.* These parameters have a first-order effect since they control the fraction of detonation momentum transferred to the plate. In the case of a square plate (used in the present work), these lengths are equal.
- *Plate material yield strength.* Not important in the rigid-plate case.
- *Array of other strength parameters for plate material.* Not important in the rigid-plate case.
- *Plate material equivalent strain/ductility.* Not important in the rigid-plate case.
- *SBE plate material density.* Not important in the rigid-plate case.
- *Plate (bending) deflection.* Not applicable in the rigid-plate case.
- *Plate acceleration.* Related to the blast loading pressure and, hence, is also irrelevant.
- *Post-SBE detonation time.* The need for this quantity appears unclear, difficult to justify, and hence, is not utilized in the present analysis.
- *SBE blast released energy.* Has a first-order effect since it scales directly with the total blast impulse.
- *Circular-disc shape SBE thickness.* Is not expected to have a first-order effect.
- *Circular-disc shape charge radius.* Has a first-order effect since it controls the volume of soil overburden ejected.
- *SBE depth of burial.* Has a first-order effect since it controls the volume of soil overburden ejected.
- *SBE/plate standoff distance.* Has a first-order effect since it controls the fraction of ejected soil which impacts and transfers impulse to the target plate.
- *Ambient atmospheric pressure.* Is not expected to have a first-order effect since momentum transfer via air shock is relatively small.
- *Speed of sound in air.* Is not expected to have a first-order effect since momentum transfer via air shock is relatively small.
- *Ratio of specific heats for air.* Is not expected to have a first-order effect since momentum transfer via air shock is relatively small.
- *Density of soil.* Is not expected to have a first-order effect because the soil fracture strain (controls the onset of bubble burst and venting) and irreversible-compaction bulk modulus (controls the absorption of detonation energy by the soil surrounding the charge) play a more important role.
- *Seismic velocity.* Has a first-order effect since it controls the volume/depth of compacted soil surrounding the detonated explosive.

- *Gravitational acceleration.* Due to small charge-to-target travel times and extremely high detonation products/soil ejecta velocities, gravity is not expected to have a first-order effect.

Reformulation. Based on the discussion presented in the previous subsection, the following six parameters originally introduced by Wenzel and Hennessey (1972) are retained in the present analysis: square target-plate edge length, SBE blast released energy, circular-disc shape charge radius, SBE depth of burial, SBE/plate standoff distance, and seismic velocity. To this list, the following six new physical parameters are added:

- (1) *Total blast impulse (I).* A new quantity added to comply with impulse measurement methods employed in the present work.
- (2) *Soil fracture strain (ϵ_{fr}).* A new quantity added which controls the onset of sand-overburden bubble burst and venting. For the same type of soil, it may be related to the soil porosity and/or degree of saturation.
- (3) *Soil irreversible compaction bulk modulus (K_{ic}).* A new quantity added which controls the amount of energy absorbed by the soil directly surrounding the charge during irreversible compaction. For the same type of soil, it may be related to the soil porosity and/or degree of saturation.
- (4) *Soil porosity (α).* A new quantity added which, together with the degree of saturation, controls the maximum degree of compaction.
- (5) *Degree of saturation (β).* A new quantity added which, together with the soil porosity, controls the maximum degree of compaction.
- (6) *Explosive detonation velocity (v_{det}).* A new quantity added which controls the time of sand-overburden bubble burst.

It should be noted that the following two quantities were also initially considered:

- (1) *Initial velocity after complete momentum transfer (v).* This quantity was initially considered because it is directly related to the impulse measurement methods employed in the present work. However, since v was found to scale directly with the blast impulse, it is not used in the present analysis (to avoid redundancy).
- (2) *Plate maximum height (H).* This quantity was also initially considered because it is directly related to the impulse measurement methods employed in the present work. However, since H also scales with the blast impulse, it is not used in this analysis (to avoid redundancy).

II Terms. The 12 physical parameters identified in the previous subsections are next normalized using the following subset of three parameters (seismic velocity, standoff distance, and total explosive energy) to form a set of nine *II* terms. The mathematical formulation of these terms is provided in Table III while the corresponding scaling law is given in Table IV.

3. Experimental procedures

In this section, a brief description is provided of the experimental setups and procedures used by McAndrew (2009) and Cheeseman (2009) to generate blast total-impulse data (as a function of different soil conditions, charge configurations, charge deployment strategies, and target-plate standoff distances). These data are analyzed in the present work.

MMMS
9,3

Π Term	Physical meaning	Similarity type
$\Pi_1 = L/R$	Square plate edge length	Geometrical
$\Pi_2 = r/R$	Circular disk-shaped charge radius	Geometrical
$\Pi_3 = d/R$	Scaled depth of burial	Geometrical
$\Pi_4 = E/K_{ic}R^3$	Non-dimensional blast energy density	Material
$\Pi_5 = v_{det}/c$	Non-dimensional charge detonation velocity	Material
$\Pi_6 = Ic/E$	Non-dimensional impulse due to SBE blast	Loading
$\Pi_7 = \alpha$	Soil porosity	Material
$\Pi_8 = \beta$	Degree of saturation	Material
$\Pi_9 = \varepsilon_{fr}$	Soil fracture strain	Material

378

Table III.

Π terms controlling total impulse delivered to the target plate

Note: Please note that the six terms appearing in this table were obtained by proper non-dimensionalization of the quantities appearing in Tables I and II using E, R, and c

Symbol	Parameter	Scale factor
<i>Original parameters of Wenzel and Hennessey (1972)</i>		
L	Square target-plate edge length	λ
r	Circular-disc shape charge radius	λ
R	SBE/plate standoff distance	λ
d	SBE depth of burial	λ
c	Seismic velocity	1.0
E	SBE blast released energy	λ^3
<i>New parameters introduced in the present work</i>		
I	Total blast impulse	λ^3
ε_{fr}	Soil fracture strain	1.0
K_{ic}	Soil irreversible-compaction bulk modulus	1.0
α	Soil porosity	1.0
β	Soil degree of saturation	1.0
v_{det}	Explosive detonation velocity	1.0
<i>Parameters introduced in the present work, but not used</i>		
v	Initial velocity after complete momentum transfer	1.0
H	Plate maximum height	λ

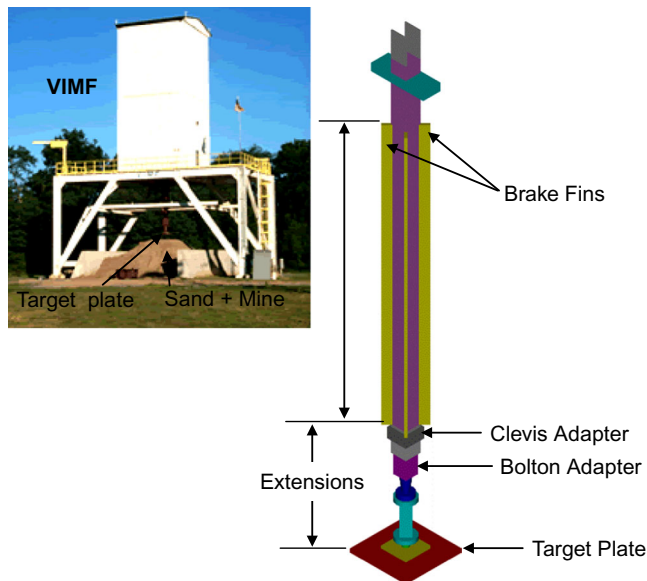
Table IV.

Replica-to-prototype scaling for impulse loading on a target plate resulting from blast of a SBE

3.1 Vertical impulse measurement facility

The Vertical impulse measurement facility (VIMF) is a structural mechanical device located at the Army Research Lab at Aberdeen Proving Ground, MD (ARL-APG) that enables direct experimental determination of the imparted blast-loading impulse via measurements of the vertical displacement of a known fixed-mass vertical guide rail that is capped with a 1.524 m \times 1.524 m \times 0.101 m steel target plate which serves as a momentum trap to capture the blast loading of the buried charge. The design and operation of the VIMF has been described in detail by Gniazdowski (2004), Skaggs *et al.* (2007) and Taylor *et al.* (2005) and will be only briefly discussed here. A schematic drawing of the VIMF including the vertical guide rail and the orientation of the charge in sand at different levels of water saturation is shown in Figure 2. A photograph of the VIMF is also given as an inset in Figure 2.

Before a VIMF test is conducted, the pit underneath the target plate is filled with sand of a given saturation level. Typically, commercially available (Quikrete) sand is



Note: The inset shows an actual photograph of the VIMF

Figure 2.
A schematic of the
vertical impulse
measurement fixture

used which consists of 94.4 percent sand, 0.3 percent gravel, and 5.3 percent silt/clay. The dry density of this sand is ca. 1.49 g/cm^3 and is typically associated with a porosity level of 0.35. To place the explosive into the sand, a circular hole is dug in the middle of the pit. After placing the explosive, the excavated sand is replaced atop the charge and compacted to form a sand overburden with a level of porosity and saturation level comparable to that of the surrounding sand. Before the charge is detonated, a probe is inserted into the soil in order to determine the saturation level.

To create the required water-saturated sand condition, a cylindrical pit 3.65 m in diameter and 1.32 m deep is first constructed in the soil within the VIMF test area. Next, approximately 14.2 m^3 of commercially available (Quikrete) sand is placed in the pit. The sand typically consists of 94.4 percent sand, 0.3 percent gravel, and 5.3 percent silt/clay. The maximum dry-sand density is 1.49 g/cm^3 while the maximum wet-sand density is 1.91 g/cm^3 .

3.2 Sandbox test facility

The VIMF target plate of dimensions given in the previous section represents a $\frac{1}{4}$ to $\frac{1}{2}$ -model of a typical military vehicle hull. To generate impulse results for smaller-scale models, the sandbox test facility at ARL is used. Essentially, the sandbox facility is a smaller and less elaborate detonation-impulse measurement facility than the VIMF with typical target plate dimensions of $0.750 \text{ m} \times 0.750 \text{ m} \times 0.0127 \text{ m}$.

4. Results and discussion

In this section, a summary and a discussion are first presented of two sets of results. The first set of results pertains to the blast-impulse measurements carried out using the VIMF

or the sandbox test facilities. The second set of results pertains to the soil property testing results obtained in our prior work (Grujicic *et al.*, 2006, 2007, 2008a, b, c, d, 2009, 2010) which were used to assess the effect of soil conditions (primarily porosity and the degree of saturation) on the key soil properties (the seismic velocity, the irreversible-compaction bulk modulus, and the strain to fracture). Based on these results and a physical-level analysis of the key phenomena/processes associated with detonation of SBEs and with interactions between the detonation products and the surrounding soil as well as with interactions between the detonation products and soil ejecta with the target, a functional relation is proposed for the non-dimensional blast impulse. Finally, a multiple-regression linear analysis is employed to parameterize this relation.

4.1 Representation and overview of the experimental results

In this section, a brief summary and overview of the experimental data generated in McAndrew (2009), Cheeseman (2009) using the VIMF and sandbox test facilities are given. The overview encompassed two sets of VIMF experimental data (McAndrew, 2009; Cheeseman, 2009) and one set of sandbox experimental data (McAndrew, 2009). Due to concerns regarding the potential misuse of the data, quantitative aspects of these data are not shown in their entirety. Instead, the data are described in more qualitative and physically-based terms.

The first set of the VIMF-measured blast-impulse data was obtained over a range of soil moistures between zero to 20 percent, a range of standoff distances from 0.4 to 1.45 m and a range of charge masses from 0.5 to 6.0 kg. All remaining charge parameters such as charge type (TNT), shape (circular disk with a 3:1 diameter-to-height ratio), and depth of burial (0.102 m) were kept constant.

The second set of the VIMF-measured blast-impulse data was obtained by varying, over two levels, the following four parameters, where the two levels are specified within parentheses:

- (1) charge standoff distance (0.3556 and 0.4064 m);
- (2) charge mass (2 and 4.45 kg);
- (3) charge depth of burial (0.0762 and 0.1016 m); and
- (4) target plate area (1.486 and 3.251 m²).

As far as the soil moisture is concerned, it was varied over three (0, 8 and 16 percent) levels.

The sandbox blast-impulse data were obtained by varying the charge mass over two levels (0.25 and 0.5 kg) and the standoff distance over five levels (0.193, 0.2007, 0.2032, 0.2286 and 0.3048 m), while the moisture content was held constant at a nominal level of 5 percent. Multiple tests were carried out at the same charge-mass/standoff-distance conditions to reveal the associated impulse variance.

Examination of the three sets of impulse data revealed that:

- As expected, detonation impulse increases with increasing charge mass.
- Detonation impulse decreases significantly with increasing standoff distance as a result of the detonation energy being distributed over an expanding hemispherical shock front, resulting in a lower energy per unit area of the shock front and, hence, a lower impulse delivered to the target plate.
- The impulse transferred to the target plate increases with increasing moisture content (e.g. at a constant charge mass, depth of burial and standoff distance,

increasing the moisture content from 0 to 20 percent more than doubles the blast impulse). This finding is related to the fact that at higher moisture contents, the volume/mass of the ejected soil is larger, the soil can undergo less irreversible compaction (and, hence, absorb less detonation energy) and possesses a higher fracture strain (ductility), allowing the sand overburden to be accelerated to higher velocities by the expanding gaseous detonation products (i.e. higher soil ductility delays the onset of the overburden burst).

- As expected, as the size of the target plate increases, the impulse captured by the target plate also increases.

4.2 Derivation of the functional relationships between Π terms

In this section, an attempt is made to construct and parameterize a functional relationship between the Π terms governing the problem of detonation of SBEs and the interactions between the detonation products, soil ejecta and the target plate (under the rigid-target condition). While it is common practice in the field of dimensional analysis to construct these relations using a monomial functional form applied directly to the Π terms, such an approach typically obscures the essential physics of the attendant phenomena/processes. Instead, physical arguments and insights will be used in constructing this relationship in the present work.

The basic relationship to be derived will have the non-dimensional impulse (represented as Π_6 on the left-hand side) while the remaining Π terms listed in Table III will appear on the right-hand side. Within the present work, the terms on the right-hand side of this relation will be organized in four groups with each group accounting for a specific physical phenomenon. The four physical phenomena identified as having a first-order effect are:

- (1) the relative area of the target plate to that of the charge;
- (2) the volume of overburden sand ejected;
- (3) the energy released during detonation of a SBE; and
- (4) the energy absorbed by the sand surrounding the charge during irreversible compaction taking place prior to overburden bubble burst and venting.

The relative area of the target plate to that of the charge. This quantity controls the fraction of soil ejecta which impinges upon the target plate. Considering the fact that typically in excess of 70 percent of the total impulse transferred to the plate is the result of soil ejecta impingement upon the plate, this quantity is identified as having a first-order effect on the total impulse transferred. To account for this effect, the following simple model for the first term on the right-hand side of the Π_6 relation is proposed: $1 - \exp(-5.8(\Pi_1 - \Pi_2))$. The term $\Pi_1 - \Pi_2$ represents the target-plate overhang (i.e. the extent by which the target half-edge length exceeds the charge radius) divided by the standoff distance and the coefficient 5.8 accounts for the fact that when the $\tan^{-1}(\Pi_1 - \Pi_2)$ is about 50° , the target plate captures nearly all (i.e. 99.9 percent) of the blast impulse carried by soil ejecta (Grujicic *et al.*, 2006).

The volume of overburden sand ejected. As discussed earlier, the majority of the impulse transferred to the target plate takes place through impingement of soil ejecta upon the target-plate's strike/lower surface. Consequently, the total impulse transferred to the plate should scale with the total volume of soil ejected where overburden soil

constitutes the majority of this volume. For the circular-disc shape of the buried charge, the following relation is proposed for the second term on the right-hand side of the Π_6 relation: $\Pi_3 \Pi_2^2 \exp(1.79\Pi_8)$. The term $\Pi_3 \Pi_2^2$ represents the volume of the soil overburden divided by the third power of the standoff distance, the term $\exp(1.79\Pi_8)$ accounts for the effect of moisture content on the volume of ejected soil and the coefficient 1.79 accounts for the fact that the volume of ejected fully-saturated ($\beta = 1.0$) soil is typically about six times larger than the corresponding ejected volume of dry ($\beta = 0.0$) soil under identical explosive-charge deployment/detonation conditions (Grujicic *et al.*, 2006).

The energy released during detonation of a SBE. To construct a term pertaining to the energy released during detonation of a SBE, the approach borrowed from numerous investigations dealing with air blast (Pehrson and Bannister, 1997) is utilized in the present work. Within this approach, the total energy released by detonation is divided by a third power of the standoff distance in order to obtain a quantity which scales with the associated volumetric energy density within the hemispherical shock front at the instant when the expanding outer surface of the hemisphere reaches the target plate. The resulting E/R^3 term has units of stress and, hence, has to be non-dimensionalized by dividing it with a stress-based quantity (the irreversible compaction bulk modulus of the soil, K_{ic} , in the present work). This non-dimensionalization is proposed in order to, at least partly, include the effect of energy absorption by the soil surrounding the charge during irreversible compaction. Thus, the third term on the right-hand side of the Π_6 relation can be written as Π_4 .

The energy absorbed by the surrounding sand. It should first be recognized that a portion of the energy absorbed by the sand surrounding the charge during irreversible compaction taking place prior to overburden bubble burst and venting, $E_{absorbed}$, was already included in the third term through the use of the irreversible compaction bulk modulus. In addition to K_{ic} , the other terms affecting the energy absorbed by the soil are:

- the square of the soil volumetric strain at full compaction, $[\alpha(1 - \beta)]^2$; and
- the volume of the fully-compacted soil, which scales with the cube of the product of c and t_{burst} where t_{burst} is the post-detonation time at which the sand-overburden bubble bursts and venting takes place.

Using a simple kinematic analysis of the sand overburden-bubble evolution (driven at a velocity v_{det} by the expanding gaseous detonation products), this post-detonation time, t_{burst} , was found to be equal to $\varepsilon_{fr}^{0.5} \cdot r/v_{det}$. The fourth term on the right-hand side of the Π_6 equation is then defined as:

$$\begin{aligned} 1 - E_{absorbed}/E &= 1 - 0.5 \cdot K_{ic} \cdot [\alpha(1 - \beta)]^2 \cdot 4/3 \cdot \pi \cdot (c \cdot t)^3 / E \\ &= 1 - 2/3 \cdot \pi \cdot K_{ic} \cdot [\alpha(1 - \beta)]^2 \cdot c^3 \cdot \varepsilon_{fr}^{3/2} \cdot r^3 / [v_{det}^3 \cdot E] \\ &= 1 - 2/3 \cdot \pi \cdot \Pi_7^2 \cdot (1 - \Pi_8)^2 \cdot \Pi_2^3 \cdot \Pi_9^{3/2} / [\Pi_5^3 \cdot \Pi_4] \end{aligned}$$

Proposed expression for the non-dimensional impulse, Π_6 . Based on the aforementioned consideration of the four phenomena identified as having a first-order effect, the following general expression is originally considered for the non-dimensionalized impulse Π_6 :

$$\Pi_6 = c_1 (1 - e^{-5.8(\Pi_1 - \Pi_2)})^{c_2} (\Pi_3 \Pi_2^2 e^{1.79\Pi_8})^{c_3} (\Pi_4)^{c_4} \times \left(1 - \frac{2\pi}{3} \Pi_7^2 (1 - \Pi_8)^2 \Pi_2^3 \Pi_9^{3/2} / (\Pi_5^3 \Pi_4) \right)^{c_5} \quad (1)$$

As can be seen in this relation, the monomial form is still used but it is applied to the four physical terms identified above rather than to the individual Π terms. After carrying out a preliminary evaluation of the five coefficients, appearing in equation (1), $c_1 - c_5$, it was found that the number of independent coefficients can be reduced to three, i.e. $c_1, c_2 \sim 2 \cdot c_4, c_3, c_4, c_5 \sim c_4$. The three independent coefficients are next renamed as follows: $a_1 = c_1, a_2 = c_3, a_3 = c_4$, and the Π_6 relation re-written as:

$$\Pi_6 = a_1 (\Pi_3 \Pi_2^2 e^{1.79\Pi_8})^{a_2} \times \left[(1 - e^{-5.8(\Pi_1 - \Pi_2)})^2 (\Pi_4) \left(1 - \frac{2\pi}{3} \Pi_7^2 (1 - \Pi_8)^2 \Pi_2^3 \Pi_9^{3/2} / (\Pi_5^3 \Pi_4) \right) \right]^{a_3} \quad (2)$$

4.3 Functional relationships pertaining to the effect of soil type/condition

Equation (2) contains a number of Π terms which are directly or indirectly affected by the type and physical conditions (e.g. porosity, degree of saturation, average particle size, particle size distribution, etc.) of the soil. In the present work, the same soil type (Quikrete) was used so that the primary parameters of the soil are the porosity and the degree of saturation. Before a multiple-regression analysis can be applied to equation (2) in order to complete evaluation of the three Π_6 -functional coefficients ($a_1 - a_3$), one must provide/determine functional relationships for the soil-related parameters/ Π -terms appearing in equation (2). This was done here by utilizing the results of our CU-ARL soil-model development work reported in a series of publications (Grujicic *et al.*, 2006, 2007, 2008a, b, c, d, 2009, 2010). Based on the results obtained in that work and using a simple strength-of-materials type of analysis, the following results are obtained.

Seismic velocity. The effect of soil porosity (α) on the speed of sound in soil at two levels of saturation ($\beta = 0.0$, dry soil and $\beta = 1.0$, saturated soil) is shown in Figure 3. A simple least-squares based curve-fitting procedure was applied to the results obtained by Grujicic *et al.* (2006, 2007, 2008a, b, c, d, 2009, 2010) which yielded the following functional relationship:

$$c = c_{full-compaction} (1 - \alpha)^{4.1 - 0.3\beta} \quad (3)$$

where the sound speed at full compaction of the soil, $c_{full-compaction}$, is set to 4,620 m/s.

Irreversible-compaction bulk modulus. K_{ic} is defined as a negative rate of change of pressure with a change in the volumetric strain when the volumetric strain is associated with irreversible compaction/densification of the soil. K_{ic} is assumed in the present work to be given as a degree-of-saturation (β) weighted average of the corresponding quantities in dry soil, $K_{ic,dry}$ and $K_{ic,saturated}$. The latter two quantities are found to depend on α and β in the following ways:

$$K_{ic,dry} = K_{ic,dry,full-compaction} \exp^{-13.5\alpha} \quad (4)$$

and:

$$K_{ic,saturated} = (1 - \alpha)K_{SiO_2} + \alpha K_{H_2O} \quad (5)$$

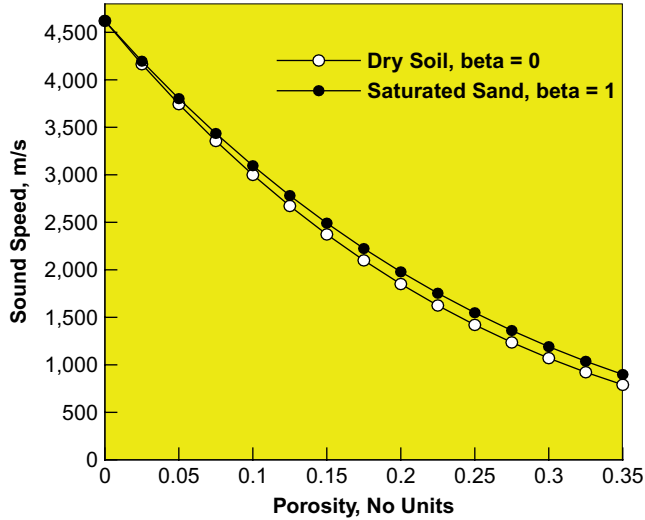


Figure 3.
The effect of soil porosity (α) and the degree of saturation (β) on the seismic velocity

where $K_{ic,dry,full-compaction}$ ($= 17.5$ GPa), K_{SiO_2} ($= 57$ GPa), K_{H_2O} ($= 2.26$ GPa), are, respectively, the irreversible-compaction bulk modulus for fully compacted dry sand, elastic compression bulk modulus of SiO_2 and elastic-compression bulk modulus of water.

The soil irreversible-compaction bulk modulus at an intermediate level of saturation is then defined as:

$$K_{ic} = (1 - \beta)K_{ic,dry} + \beta K_{ic,saturated} \quad (6)$$

The effect of porosity and the degree of saturation on the irreversible-compaction bulk modulus as defined by equation (6) is shown in Figure 4.

Fracture strain. Our prior work (Grujicic *et al.*, 2006, 2007, 2008a, b, c, d, 2009, 2010) established that while the degree of soil compaction (i.e. porosity) affects soil strength (including its fracture strength), it has no significant effect on the soil ductility (as measured by the strain to fracture). On the other hand, through capillary-enhanced inter-particle cohesion, the degree of saturation has a major effect on the soil fracture strain, Figure 5. Using the results obtained in our prior work (Grujicic *et al.*, 2006, 2007, 2008a, b, c, d, 2009, 2010), fracture strain, ϵ_{fr} , is found to depend in the following way on the degree of saturation:

$$\epsilon_{fr} = \epsilon_{fr,saturated} - (\epsilon_{fr,saturated} - \epsilon_{fr,dry})e^{-4.5\beta} \quad (7)$$

where, $\epsilon_{fr,dry}$ ($= 0.06$) and $\epsilon_{fr,saturated}$ ($= 0.11$), are the dry and saturated soil fracture strains.

4.4 Linear regression analysis

To determine the three Π_6 -functional coefficients, $a_1 - a_3$, a logarithmic mathematical operation is applied to both sides of equation (2) and a simple multi-regression linear analysis is employed to the transformed equation (2) in which both sides are evaluated using the aforementioned three sets of experimental data (McAndrew, 2009;

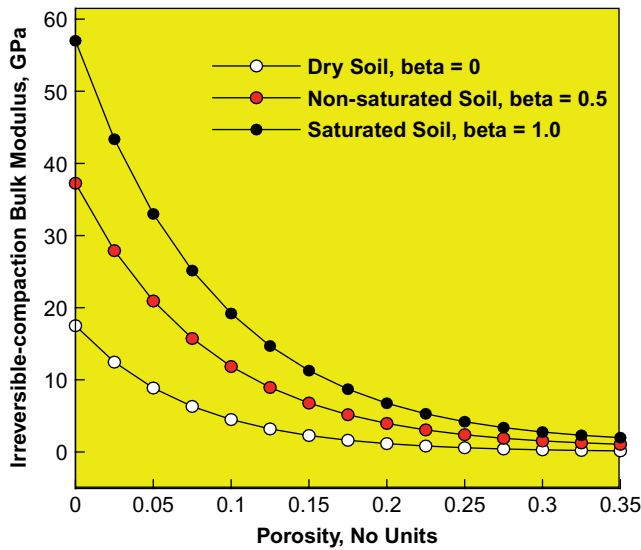
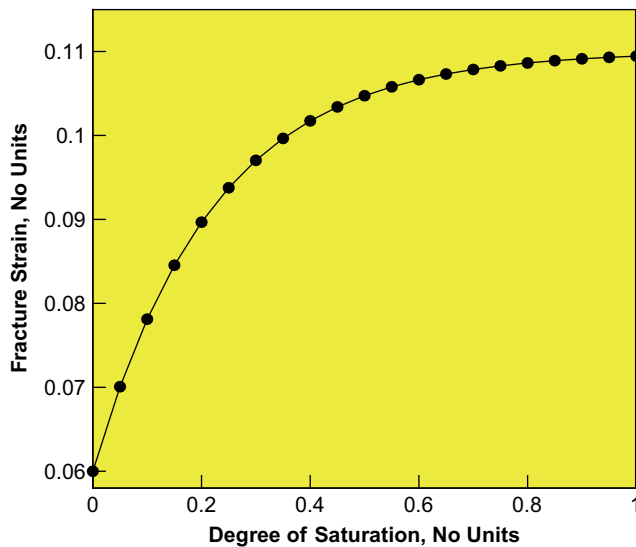


Figure 4. The effect of soil porosity (α) and the degree of saturation (β) on the irreversible-compaction bulk modulus



Note: Please note that while soil porosity (α) affects soil strength, it has no first-order effect on the soil ductility, i.e. the fracture strain

Figure 5. The effect of the degree of saturation (β) of soil on the soil fracture strain

Cheeseman, 2009). This procedure yielded the values for the three Π_6 functional coefficients, $a_1 - a_3$. However, due to previously mentioned concerns regarding the misuse of the results generated in this work, the values for these coefficients are not reported here.

An example of the results obtained in the multi-regression linear analysis is shown in Figure 6 in which a plot is given showing the correlation between measured Π_6 values and their computed counterparts. The goodness-of-fit of the measured impulses by the proposed functional relation, equation (2), is quantified by the Pearson correlation coefficient, R_{corr} , as calculated using the formula:

$$R_{corr} = \frac{1}{n-1} \sum_{i=1}^n \left(\frac{x_i - \bar{x}}{s_x} \right) \left(\frac{y_i - \bar{y}}{s_y} \right) \quad (8)$$

where $x = \Pi_6^{exp}$ and $y = \Pi_6^{comp}$ are used to denote, respectively, the measured (McAndrew, 2009; Cheeseman, 2009) and the computed (equation (2)) non-dimensional impulse values, n represents the total number of measured/computed data points, an over-bar designates the mean value, and s represents the corresponding standard deviation.

The computed value of the correlation coefficient ($R_{corr} = 0.90$) appears to be relatively small, suggesting that perhaps the proposed impulse function, equation (2), is not the most appropriate. However, before reaching this conclusion, one must account also for a relatively large range of values of the measured blast impulse under nearly identical test conditions (i.e. for the large blast-impulse variance). To help clarify this point, a few horizontal error bars are drawn in Figure 6 to denote the typical range of experimentally-measured Π_6 values obtained under almost identical test conditions. Since in most cases, the Π_6^{comp} vs Π_6^{exp} correlation line intersects these error bars, one should conclude that despite a relatively low value of the correlation coefficient, the proposed blast-impulse function, equation (2), appears appropriate. This conjecture is further supported by a finding that if the individual Π_6^{exp} values associated with the nearly-identical test conditions are replaced with their respective mean values, the value of the correlation coefficient increases to $R_{corr} = 0.94$. It should also be pointed out that

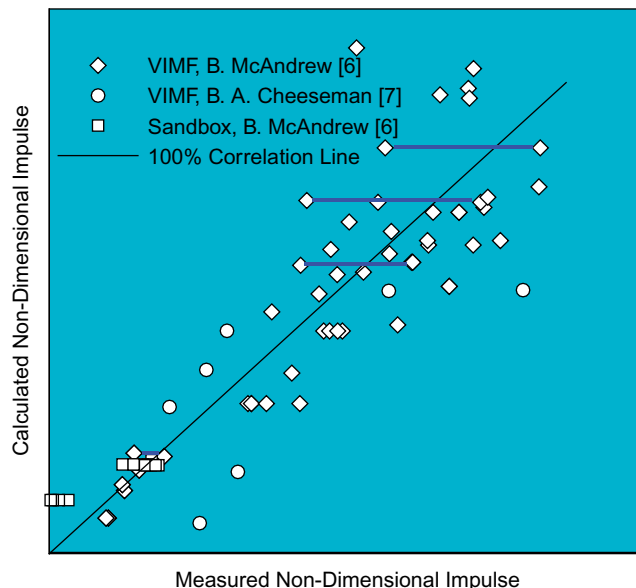


Figure 6.
A correlation analysis between the measured non-dimensional blast impulse data and their corresponding computed values obtained using the dimensional analysis developed in the present work

some of the VIMF data were obtained for the case of a V-shaped target plate. Since the analysis carried out in the present work assumed that the target plate is flat, the experimental results in question are not expected to correlate well with the proposed Π_6 relation. This expectation was confirmed by the finding that the correlation coefficient increased from 0.90 to 0.92 when the experimental data corresponding to the V-shaped target plate were not considered in the multiple-regression linear analysis.

To quantitatively validate the scaling aspect of the dimensional analysis carried out in the present work, a multiple-regression linear analysis case was also considered in which only the VIMF data were used. This procedure yielded a correlation coefficient $R_{corr} = 0.92$. Since this value is somewhat higher than the value $R_{corr} = 0.90$ (based on the consideration of both the VIMF and sandbox results), one may question the validity of the present scaling analysis. However, one must also take into consideration the fact that in most cases, the “rigid-plate” condition was not satisfied for the sandbox facility experiments. While target plate deflections are typically assumed to not alter the magnitude of the blast load (Wenzel and Hennessey, 1972), they may seriously affect the accuracy with which the blast impulse is measured. In fact, it was found that leaving out a few of the “outlier” sandbox data points can make the difference between the two values of the correlation coefficient smaller than 0.005.

4.5 Application of the proposed Π_6 relation

In the previous section, it was established that the proposed Π_6 relation can reasonably well account for the observed effects of various soil conditions, charge configurations, charge deployment strategies and vehicle ground clearances on the measured blast impulse values. In this section, a brief description is provided regarding the application of the Π_6 relation, equation (2). In assessing impulse loads experienced by a target structure during a fully-described landmine blast scenario, the following procedure should be utilized:

- All parameters listed in Table II which pertain to the explosive charge and charge/plate positioning must first be specified.
- Next, the three soil parameters appearing in Table II (i.e. seismic velocity, soil fracture strain and soil irreversible-compaction bulk modulus) must be defined. However, as implied by the results in Figures 3-5, the values of these parameters depend upon both the soil porosity (α) and degree of saturation (β). In other words, the values of these parameters can be established only after α and β are determined. The three soil parameters mentioned above can then be found using the correlation curves shown in Figures 3-5. Thus, in order to utilize Figures 3-5 and calculate the expected impulse from the resulting soil parameter values, α and β must be quantified.
- To determine α and β , sand/soil mass density (ρ) and the volumetric moisture content (w) of the sand/soil must be first determined experimentally. Then, the density, $\rho = (1 - \alpha)\rho_{full-compaction} + \alpha\beta\rho_{H_2O}$, and the volumetric moisture content, $w = \alpha\beta$, relations are used to compute α and β . For convenience, functional relationships between α and β on one side and ρ and w on the other are determined for a standard value of $\rho_{full-compaction} = 2,670 \text{ kg/m}^3$ and $\rho_{H_2O} = 1,000 \text{ kg/m}^3$ and depicted, respectively, in Figures 7 and 8; and
- Once α and β (and, in turn, c , K_{ic} , and ε_{fr}) are evaluated, the total impulse can be computed from equation (2) as:

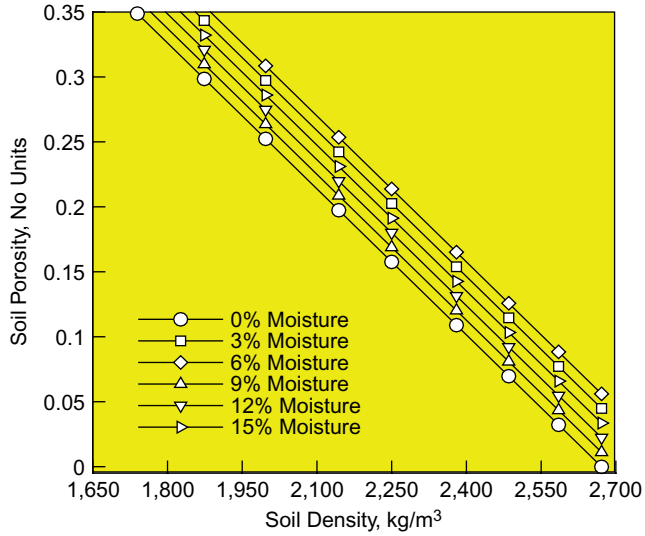


Figure 7.
A correlation between soil porosity and its density and moisture content

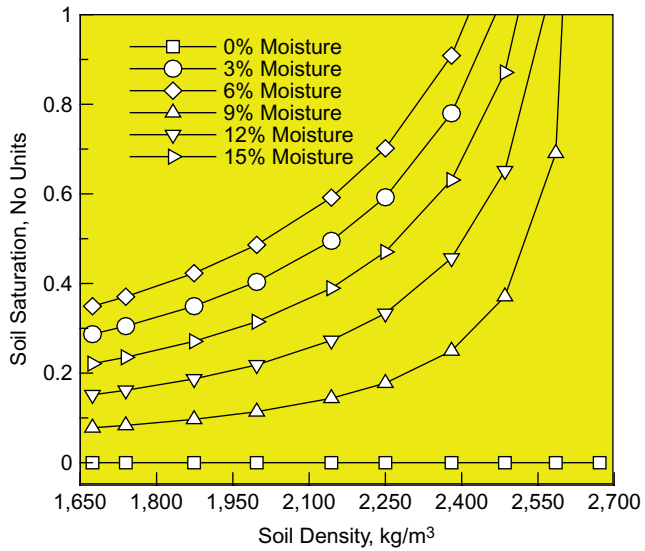


Figure 8.
A correlation between soil saturation-level and its density and moisture content

$$I = \frac{E}{c} a_1 \left(\left(\frac{d}{R} \right) \left(\frac{r}{R} \right)^2 e^{1.79\beta} \right)^{\alpha_2} \times \left[\left(1 - e^{-5.8(L-r)/R} \right)^2 \left(\frac{E}{K_{ic} R^3} \right) \left(1 - \frac{(2\pi/3)\alpha^2(1-\beta)^2(r/R)^3 \epsilon_{fr}^{3/2}}{(v_{det}/c)^3 (E/K_{ic} R^3)} \right) \right]^{\alpha_3} \quad (9)$$

5. Summary and conclusions

Based on the results obtained in the present work, the following main summary points and conclusions can be made:

- A detailed overview and critical assessment is provided of the dimensional analysis proposed by Wenzel and Hennessey (1972) for sizing military vehicle hulls required to survive different levels of blast loads associated with detonation of SBEs.
- Using basic physical-level understanding of the key phenomena associated with SBE detonation and the interaction of detonation products with the surrounding soil as well as the interactions of detonation products and soil ejecta with the target plate (a surrogate for the vehicle hull), it was found that the original analysis of Wenzel and Hennessey (1972) can be greatly simplified if it is based on the physical phenomena/processes which have a first-order effect.
- A new set of non-dimensional Π terms is introduced which not only accounts for the effects of target-plate/explosive charge geometries, materials used, deployment strategies, and also include critical effects associated with the soil type and structural-condition/consistency.
- A new functional relationship is introduced which relates the blast impulse to the geometrical, material, and deployment aspects of the explosive charge and target plate as well as of the soil into which the explosive is buried.
- A set of blast-impulse experimental data is finally used to parameterize this relation and judge its appropriateness.

References

- Buckingham, E. (1914), "On physically similar systems; illustrations of the use of dimensional equations", *Physical Review*, Vol. IV, pp. 345-376.
- Cheeseman, B.A. (2009), ARL-APG Private Communication.
- Gniazdowski, N. (2004), "The vertical impulse measurement facility maintenance and inspection manual", ARL Technical Report (in submission).
- Grujicic, M., Pandurangan, B. and Cheeseman, B.A. (2006), "The effect of degree of saturation of sand on detonation phenomena associated with shallow-buried and ground-laid mines", *Shock and Vibration*, Vol. 13, pp. 41-62.
- Grujicic, M., Pandurangan, B., Summers, J.D., Cheeseman, B.A. and Roy, W.N. (2008a), "Application of the modified compaction material model to soil with various degrees of water saturation", *Shock and Vibration*, Vol. 15, pp. 79-99.
- Grujicic, M., Pandurangan, B., Coutris, N., Cheeseman, B.A., Roy, W.N. and Skaggs, R.R. (2008b), "Computer-simulations based development of a high strain-rate, large-deformation, high-pressure material model for STANAG 4569 sandy gravel", *Soil Dynamics and Earthquake Engineering*, Vol. 28, pp. 1045-1062.
- Grujicic, M., Pandurangan, B., Coutris, N., Cheeseman, B.A., Roy, W.N. and Skaggs, R.R. (2009), "Derivation and validation of a material model for clayey sand for use in landmine detonation computational analysis", *Multidiscipline Modeling in Materials and Structures*, Vol. 5, pp. 311-344.
- Grujicic, M., Pandurangan, B., Coutris, N., Cheeseman, B.A., Roy, W.N. and Skaggs, R.R. (2010), "Derivation, parameterization and validation of a sandy-clay material model for use in landmine detonation computational analyses", *Journal of Materials Engineering and Performance*, Vol. 10, pp. 434-450.

- Grujicic, M., Pandurangan, B., Huang, Y., Cheeseman, B.A., Roy, W.N. and Skaggs, R.R. (2007), "Impulse loading resulting from shallow buried explosives in water-saturated sand", *Journal of Materials: Design and Applications*, Vol. 221, pp. 21-35.
- Grujicic, M., Pandurangan, B., Mocko, G.M., Hung, S.T., Cheeseman, B.A., Roy, W.N. and Skaggs, R.R. (2008c), "A combined multi-material Euler/Lagrange computational analysis of blast loading resulting from detonation of buried landmines", *Multidiscipline Modeling in Materials and Structures*, Vol. 4, pp. 105-124.
- Grujicic, M., Pandurangan, B., Qiao, R., Cheeseman, B.A., Roy, W.N., Skaggs, R.R. and Gupta, R. (2008d), "Parameterization of the porous-material model for sand with different levels of water saturation", *Soil Dynamics and Earthquake Engineering*, Vol. 28, pp. 20-35.
- McAndrew, B. (2009), ARL-APG Private Communication.
- Pehrson, G.R. and Bannister, K.A. (1997), "Airblast loading model for DYNA2D and DYNA3D", ARL Technical Report.
- Skaggs, R.R., Watson, J., Adkins, T., Gault, W., Canami, A. and Gupta, A.D. (2007), "Blast loading measurements by the vertical impulse measurement fixture (VIMF)", ARL Technical Report-3383, US Army Research Laboratory, Aberdeen Proving Ground, Aberdeen, MD.
- Taylor, L.C., Skaggs, R.R. and Gault, W. (2005), "Vertical impulse measurements of mines buried in saturated sand", *Fragblast*, Vol. 9, pp. 19-28.
- Wenzel, A. and Hennessey, J.M. (1972), "Analysis and measurements of the response of armor plates to land mine attacks", *Proceedings of the Army Symposium on Solid Mechanics, Warren, MI*, pp. 114-128.

About the authors

Mica Grujicic is a Professor, Mechanical Engineering, Clemson University. Mica Grujicic's research interests include computational engineering.

Patrick Glomski is a PhD student, Mechanical Engineering, Clemson University. His research interests include finite element analysis.

Bryan Cheeseman is a Research Engineer, Research Labs, Aberdeen Proving Ground. Bryan Cheeseman's research interests include blast modeling and simulation.